

Supraglacial river forcing of subglacial water storage and diurnal ice sheet motion

L.C. Smith^{1,2,3}, L.C. Andrews⁴, L.H Pitcher^{5,3}, B.T. Overstreet⁶, Å.K. Rennermalm⁷, M.G. Cooper^{3,8}, S.W. Cooley^{9,3}, J.C. Ryan¹, C. Miège^{7,10}, C. Kershner^{11,13}, C.E. Simpson^{12,3}

¹Institute at Brown for Environment and Society (IBES), Brown University, Providence, Rhode Island, 02912, USA

²Department of Earth, Environmental, and Planetary Sciences, Brown University, Providence, Rhode Island, 02912, USA

³Department of Geography, University of California - Los Angeles, Los Angeles, California, 90095, USA

⁴ Global Modeling and Assimilation Office, NASA Goddard Space Flight Center, Greenbelt, Maryland, 20771, USA

⁵Cooperative Institute for Research in Environmental Sciences (CIRES), University of Colorado – Boulder, Boulder, Colorado, 80303, USA

⁶Department of Geology and Geophysics, University of Wyoming, Laramie, WY, 82071, USA

⁷Department of Geography, Rutgers, The State University of New Jersey, New Brunswick, 08901, New Jersey

⁸Atmospheric Sciences and Global Change Division, Pacific Northwest National Laboratory, Richland, Washington, 99352, USA

⁹Department of Earth System Science, Stanford University, Stanford, CA, 94305 Affiliation for author 9.

¹⁰Department of Geography, University of Utah, Salt Lake City, Utah, 84112, USA

¹¹Research Directorate, National Geospatial-Intelligence Agency, Springfield, VA 22150

¹²RedCastle Resources, Inc., Salt Lake City, Utah, 84138, USA

¹³Department of Geography and Geoinformation Science, George Mason University, Fairfax, VA 22030

Corresponding author: Laurence Smith (laurence_smith@brown.edu)

Key Points:

- We present coincident field measurements of supraglacial river discharge and ice sheet motion on the southwest Greenland ablation zone
- The measurements are obtained upstream of a major moulin, enabling study of how supraglacial meltwater runoff influences subglacial hydrology and ice motion

- 36 ● Recorded ice velocities are strongly correlated with measurements of supraglacial river
37 discharge acquired hourly over the 7-day study period
- 38 ● Differencing of supra- and proglacial discharge hydrographs suggests that diurnal
39 fluctuations in subglacial water storage drive short-term variations in ice motion

40

41 **Key Points**

- 42 ● We measure supraglacial river discharge entering a major moulin simultaneously with
43 local accelerations in ice sheet motion
- 44 ● Recorded ice speeds are strongly correlated with diurnal cycles of moulin input over the
45 7-day field experiment period
- 46 ● Differencing supra- and proglacial hydrographs suggests diurnal fluctuations in
47 subglacial water storage drive short-term ice motion

48

49 **Abstract (150 words max)**

50 Surface melting impacts ice sheet sliding by supplying water to the bed, but subglacial processes
51 driving ice accelerations are complex. We examine linkages between surface runoff, transient
52 subglacial water storage, and short-term ice motion from 168 consecutive hourly measurements
53 of meltwater discharge (moulin input) and GPS-derived ice surface motion for Rio Behar, a ~60
54 km² moulin-terminating supraglacial river catchment on the southwest Greenland Ice Sheet.
55 Short-term accelerations in ice speed correlate strongly with lag-corrected measures of
56 supraglacial river discharge ($r=0.9$, $\rho=0.7$, $p<0.01$). Though our 7-day record cannot address
57 seasonal-scale forcing, diurnal ice accelerations align with normalized differenced supraglacial
58 and proglacial discharge, a proxy for subglacial storage change, better than GPS-derived ice
59 surface uplift. These observations counter theoretical steady-state basal sliding laws and suggest
60 that moulin- and proglacially induced fluctuations in subglacial water storage, rather than
61 absolute subglacial water storage, drive short-term ice accelerations.

62

63 **Plain Language Summary**

64 The importance of surface meltwater runoff to Greenland ice sheet subglacial hydrology and ice
65 sliding dynamics is widely recognized but poorly constrained by field observations. We present
66 168 consecutive hours of rare in-situ discharge measurements in a large supraglacial river
67 draining the ice sheet surface, just upstream of where it plummets into a major moulin. GPS
68 measurements of ice surface motion record brief accelerations in ice sliding speed that follow
69 daily cycles in meltwater entering the moulin. By comparing these measurements with
70 proglacial river discharges leaving the ice sheet, we identify daily fluctuations in subglacial
71 water storage that track short-term accelerations in ice motion. These findings affirm the
72 importance of supraglacial rivers to subglacial water pressure and ice dynamics, even in
73 relatively thick ice >40 km inland from the ice terminus.

74

75 1. Introduction

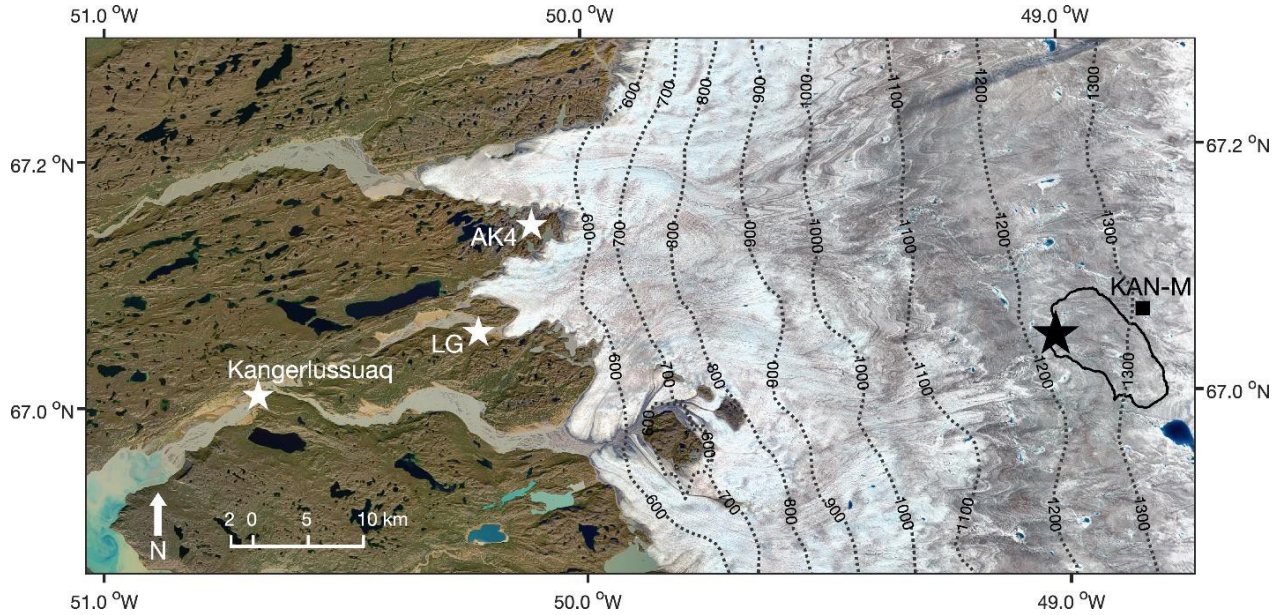
76 Accurate models of ice-sheet response to climate change require good physical
77 understanding of interactions between surface melting, subglacial hydrology, and ice dynamics
78 (e.g., *Bell, 2008; Chu, 2014; Davison et al., 2019*). On the Greenland Ice Sheet (GrIS) ablation
79 zone, surface melting activates a perennial hydrologic system of supraglacial streams, rivers, and
80 lakes (*Irvine-Fynn et al., 2011; Rennermalm et al., 2013a; Lampkin and VanderBerg, 2014;*
81 *Pitcher and Smith, 2019*), which commonly drain into moulins forming a dynamic subglacial
82 drainage system that modifies basal pressures and ice motion (e.g. *Zwally et al., 2002; Van de*
83 *Wal et al., 2008; Bartholomew et al., 2012; Meierbachtol et al., 2013*). While early concerns
84 about warming-induced runaway sliding now seem unfounded (e.g. *Tedstone, et al., 2013;*
85 *2015; van de Wal et al., 2015; Flowers, 2018*), physical processes linking GrIS supraglacial
86 meltwater runoff, ice sheet basal pressures, and ice sliding remain under intense study (*Nienow et*
87 *al., 2017; Davison et al., 2019; Williams et al. 2020*), particularly processes governing englacial
88 connectivity and subglacial evolution due to surface melting (e.g. *Poinar et al., 2015; Stevens et*
89 *al., 2015; Christoffersen et al., 2018*).

90 Traditional basal sliding law formulations linking subglacial pressure and ice motion
91 assume steady-state basal cavities (e.g. *Bindschadler, 1983; Schoof, 2005; Gagliardini et al.,*
92 *2007*). However, observational research suggests that cavities constantly undergo transient
93 evolution in response to fluctuations in supraglacial meltwater supply and subglacial
94 channelization (*Iken et al., 1983; Bartholomew et al., 2008; Hoffman et al., 2011; Cowton et al.,*
95 *2016; Andrews et al., 2018*). If so, highest subglacial water pressures (and therefore ice sliding
96 speeds) should occur when transient cavities are growing fastest, not when they are largest (*Iken*
97 *et al., 1983; Cowton et al., 2016*).

98 Evidence for transient cavity evolution is drawn primarily from GPS-derived correlations
99 of horizontal ice speed with vertical ice surface uplift (interpreted as a proxy for total subglacial
100 water storage, S) or its first derivative (interpreted as subglacial water storage rate-of-change,
101 $L'S$). GrIS horizontal ice sliding speed broadly covaries with vertical surface uplift over seasonal
102 time scales (e.g., *Bartholomew et al., 2010; 2012; Hoffman et al., 2011*), but variations at shorter
103 timescales tend to correlate better with its derivative (*Hoffman et al., 2011; Cowton et al., 2016;*
104 *Andrews et al., 2018*). Such correlations are typically weak and spatially variable due to a range
105 of factors confounding estimation of basal uplift from ice surface elevation measurements
106 (*Hoffman et al., 2011; Andrews et al., 2018*). Therefore, it is difficult to infer interactions
107 between surface melting, subglacial water storage, cavity growth, and ice motion for the GrIS,
108 despite previous success on mountain glaciers (e.g. *Bartholomew et al., 2008; 2011; Armstrong*
109 *and Anderson, 2020*)

110 To study the links among supraglacial runoff, subglacial water storage fluctuations, and
111 short-term ice motion, we present in situ measurements of moulin input (i.e. supraglacial
112 discharge), ice surface speed, and ice surface uplift for Rio Behar, a large supraglacial river on
113 the GrIS mid-elevation (>1200 m a.s.l.) ablation zone (**Figure 1**). We compare daily cycles in
114 these variables with PROMICE automated weather station (AWS) measurements of surface
115 energy balance and ablation (*Fausto and van As, 2019*), and with proglacial river discharges
116 from three gauging stations downstream (*Rennermalm et al., 2017; Tedstone et al., 2017; van As*
117 *et al., 2019*). We present GPS measurements of horizontal ice surface speed and vertical uplift,
118 and use them to estimate subglacial storage S and rate-of-change $L'S$, respectively. We also
119 compute alternate proxies for S and $L'S$ by differencing normalized supraglacial and proglacial

120 discharge hydrographs (adapted from *Bartholomaeus et al., 2008, 2011; McGrath et al., 2011;*
121 *Armstrong and Anderson, 2020*). We conclude that diurnal cycles in supraglacial river discharge
122 drive ice accelerations through L'S, confirming that transient water storage and cavity growth are
123 important influences on GrIS subglacial basal pressure and short-term ice motion.
124
125



126
127 **Figure 1: Study area in southwest Greenland. Black star shows location of our GPS measurements of ice surface**
128 **motion and Acoustic Doppler Current Profiler (ADCP) measurements of moulin input (supraglacial discharge) in**
129 **Rio Behar, a large supraglacial river penetrating the ice sheet >40 km from the ice edge. Field work was**
130 **conducted ~750 m upstream of the Rio Behar terminal moulin. Black outline delineates the surface catchment**
131 **(60.02 km² in July 2016). White stars locate proglacial river gauging stations; black square locates PROMICE**
132 **KAN_M automated weather station. Background is a 26 July 2016 true-color Landsat-8 satellite image.**

133

134 2. Data and Methods

135 2.1 Observational data

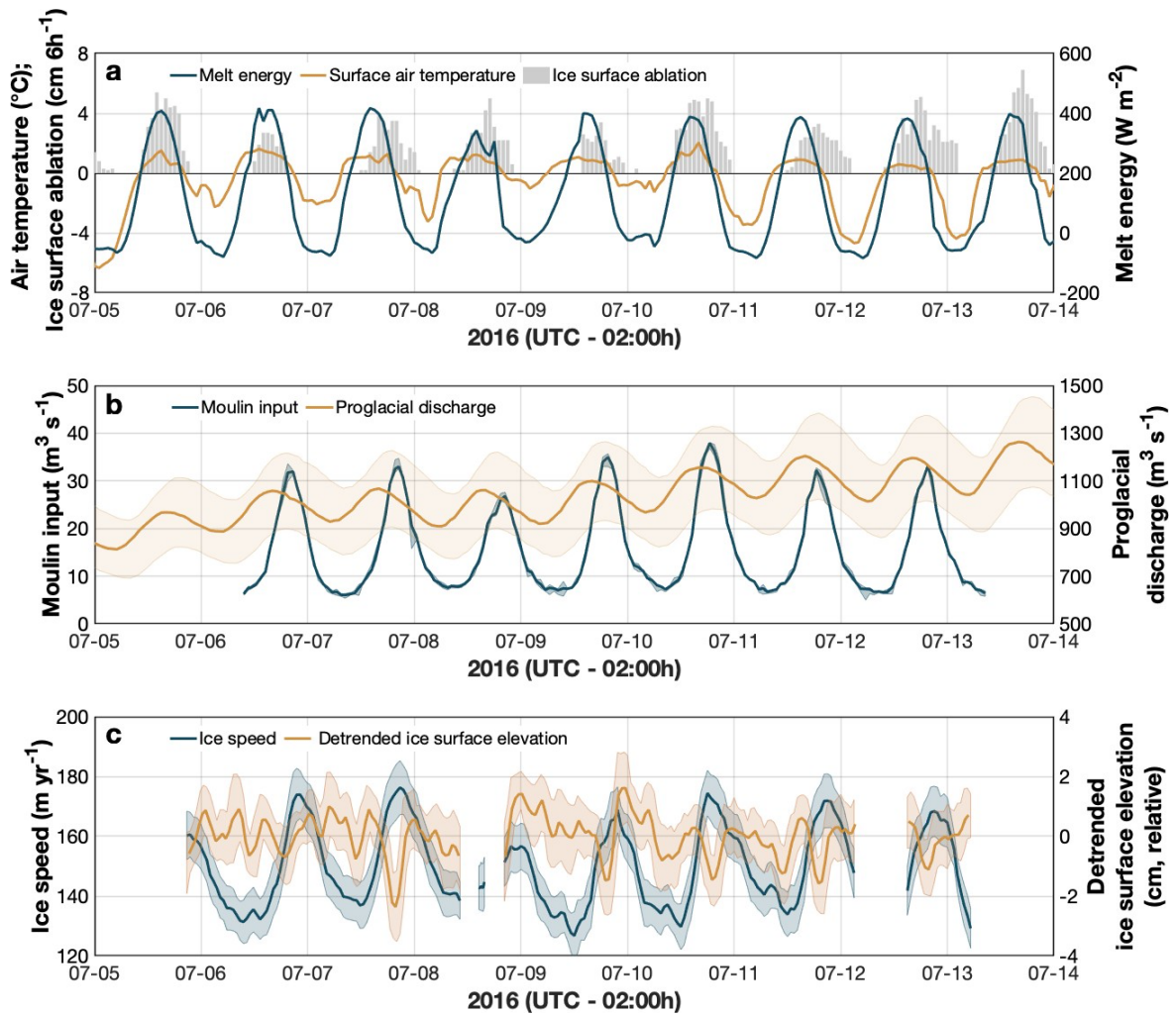
136 In July 2016 the Rio Behar terminal moulin was located at 67.047°N, -49.033°W, with an
137 upstream drainage catchment of ~60.2 km² and mean surface elevation >1200 m (**Figure 1**). We
138 established a field camp to measure moulin meltwater input and ice surface motion ~750 m
139 upstream (~67.050°N, -49.018°W). During 5-13 July 2016 we collected 174 measurements of
140 supraglacial river discharge using a SonTek RiverSurveyor M9 Acoustic Doppler Current
141 Profiler (ADCP) and methods of *Smith et al. (2017)*. A Tyrolean cableway was suspended over
142 the river to safely and repeatedly tow the ADCP back and forth across the channel every hour
143 (**Figures S1-S4**). In total 847 ADCP transects were acquired, of which 677 later passed rigorous

144 quality-assurance screening and were used to compute 168 consecutive hourly discharge
145 measurements from 6-13 July (**Text S1-S3, Figure S5, Tables S1-S2, Datasets S1-S2**).

146 Simultaneous measurements of ice surface motion were collected every 5-s using a
147 Trimble R7 GPS receiver and Trimble Zephyr Geodetic antenna anchored 3m into the ice to
148 prevent its movement from ablation (67.048°N, -49.018 °W, elevation 1211.43 m). On-ice
149 kinematic GPS positions were later estimated using carrier-phase differential processing relative
150 to a bedrock mounted base station (~47 km baseline, 67.150°N, -50.058°W, elevation 581.19)
151 and final International GNSS Service satellite orbits (*Chen, 1998; Estey and Meertens, 1999;*
152 *Hoffman et al., 2011; Andrews et al. 2014; 2018; Text S4*). To assess surface melt processes,
153 simultaneous measurements of 2-m air temperature, energy balance, and ablation were obtained
154 from the nearby PROMICE KAN_M AWS (*Fausto and van As, 2019, Text S5*). Proglacial river
155 discharges were obtained from gauges at Qinguata Kuussua/Watson River in Kangerlussuaq
156 (*van As et al., 2019*), its northern tributary Akuliarusiarsuup Kuua (AK4) near the ice terminus
157 (*Rennermalm et al., 2017, AK4 station*), and a discontinued gauge near Leverett Glacier
158 (*Tedstone et al., 2017*) (**Figure 1**). Lagged correlation coefficients (e.g. *Flowers et al., 2016;*
159 *Armstrong and Anderson, 2020*) were used to quantify links between these variables and GPS-
160 derived ice motion, and to compute proglacial timing delays between the ice edge and
161 Kangerlussuaq (**Text S6, S8**).

162 2.2 Proxies for S and ΔS

163 GPS-derived vertical positions and their first derivative were used to estimate subglacial
164 storage S and rate-of-change ΔS (e.g. *Bartholomew et al., 2012; Cowton et al., 2016; Text S7*).
165 Proxies for S and ΔS were also computed by adapting a meltwater input-output approach
166 (*Bartholomew et al. 2008; 2011; McGrath et al. 2011; Armstrong and Anderson, 2020*)
167 comparing relative timings of supra- and proglacial river discharge hydrographs (**Text S7**).
168 Hydrographs were normalized and differenced (supraglacial minus proglacial) to assess their
169 relative timings and shapes at Rio Behar moulin and at the ice edge. These "discharge-
170 difference" proxies are unitless and do not satisfy mass conservation. They characterize
171 instantaneous net water storage changes, not subglacial routing delays and/or storages known to
172 retard proglacial discharges longer than 24 h (e.g. *Chandler et al., 2013; Rennermalm et al.,*
173 *2013b; Smith et al., 2015; Chu et al., 2016; van As et al., 2017; Pitcher et al. 2020*). From dye
174 tracing experiments, subglacial routing from ~1300 m elevation takes 1-3 days (*Chandler et al.*
175 *2013, site L57*), or ~2-5 days from proglacial hydrograph analysis (*van As et al., 2017*). Such
176 subglacial delays and storages are irrelevant to our purpose here, which is simply to characterize
177 instantaneous subglacial conditions at our field site, not Lagrangian transport to the ice edge.
178 Descriptions of all data, methods, and uncertainties are presented in **SI (Text S1-S9, Figures S7-**
179 **S14, Tables S1-S5)**.



180
 181 **Figure 2:** In situ measurements of (a) melt energy, air temperature, and ice ablation from KAN_M; (b) Rio Behar
 182 moulin input (supraglacial discharge) and proglacial discharge; (c) ice surface speed and elevation. Colored
 183 envelopes (b, c) represent measurement uncertainties.

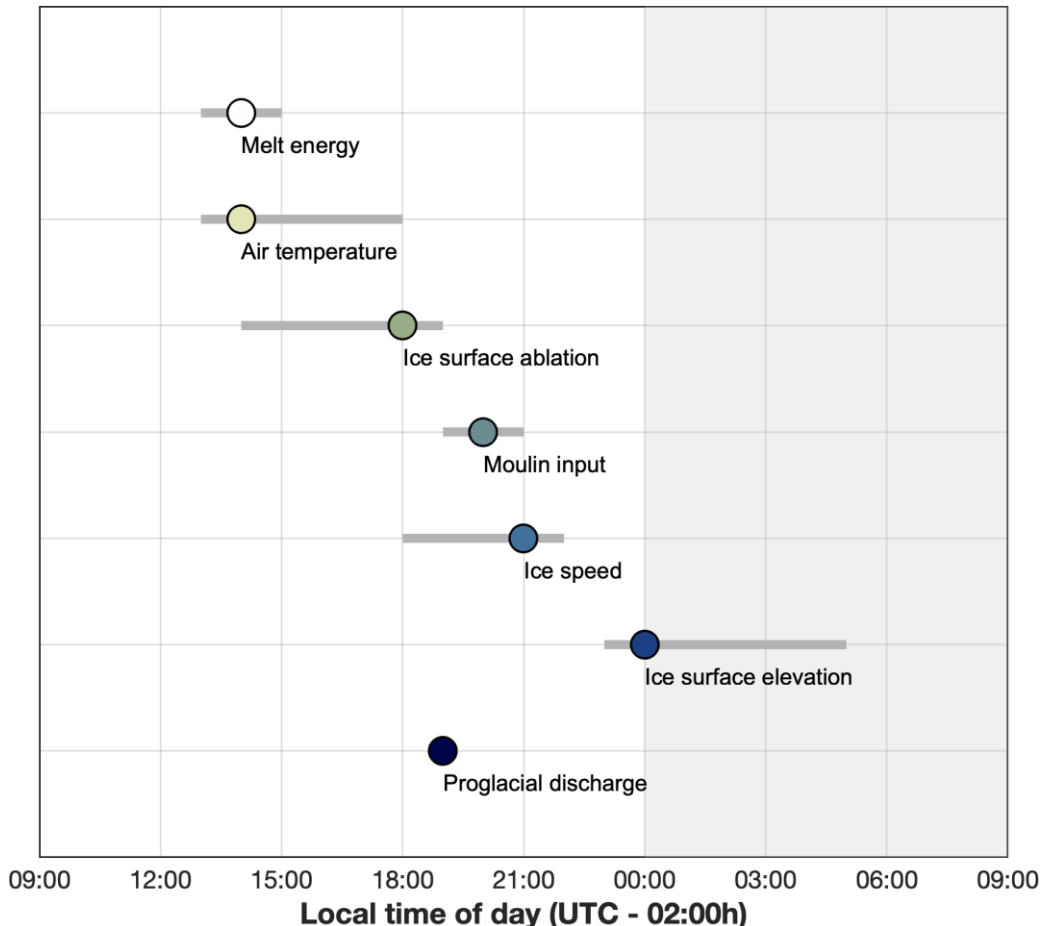
184

185 3. Results

186 3.1 Correlations of ice speed with other variables

187 We find strong diurnal cycles in all variables except surface elevation, with daily
 188 accelerations in horizontal ice speed closely tracking moulin input and melt energy (**Figure 2;**
 189 **Table S3**). A consistent progression is observed in the timing of daily peaks, with melt energy
 190 and air temperatures peaking near local solar noon, followed by sequential peaks in ice ablation,
 191 moulin input, ice speed, and proglacial discharge (**Figure 3**). The timing of daily peaks is most
 192 consistent for melt energy, moulin input, ice speed, and proglacial discharge, whereas peaks in
 193 air temperature, ablation, and especially ice surface elevation are more variable as indicated by

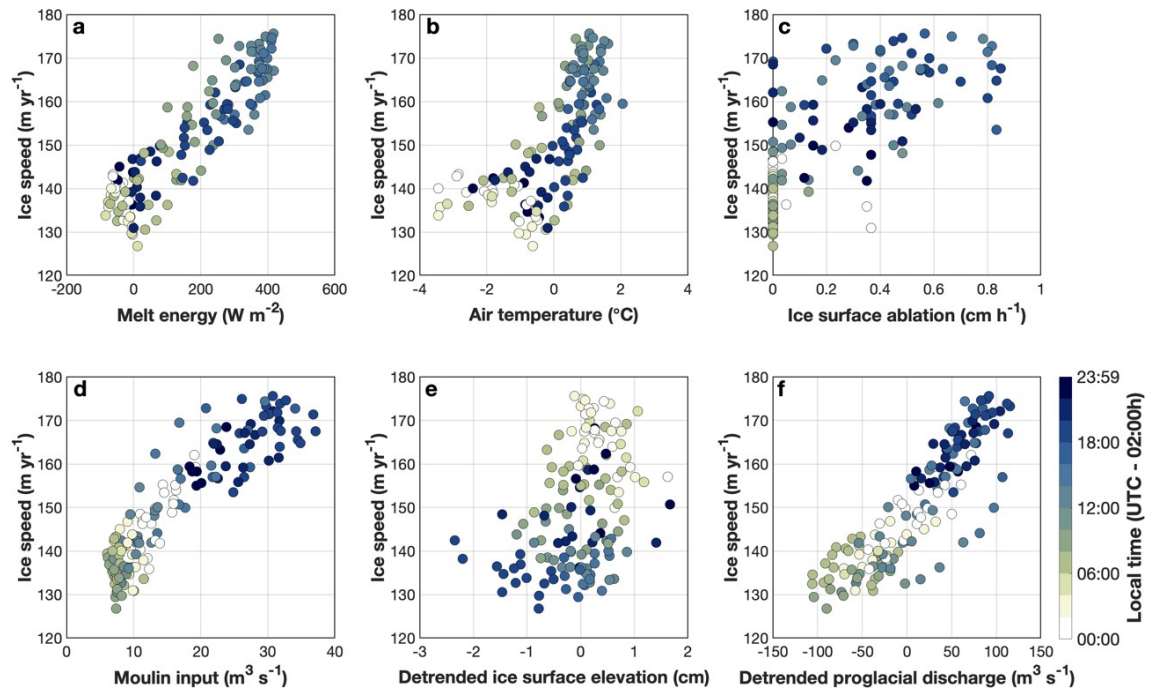
194 their peak timing range (Table S3).



195
196 **Figure 3: Mean daily peak timing (circles) and timing range (grey bars) of observed variables. Diurnal cycles in**
197 **melt energy and air temperatures peak around solar noon, followed by peaks in ice ablation, proglacial**
198 **discharge, moulin input, ice speed, and ice surface uplift. GPS-derived daily peaks in uplift are temporally**
199 **variable (Table S3). Peak proglacial discharge has little timing variability and is shifted -5h earlier to account for**
200 **the timing offset between Kangerlussuaq and the ice edge. This figure presents only the timing of daily peaks,**
201 **not subglacial routing delays and/or storages of meltwater.**
202

203 After lagging our GPS-derived horizontal ice speed time-series to correct for its mean
204 timing offsets with the other variables, we compute correlations between potential forcing
205 variables and ice speed using Pearson's r , which assumes a linear relationship, and Mann-
206 Kendall's τ , which does not assume a linear relationship between variables. We find that ice
207 speed correlates strongly with moulin input ($r=0.90$, $\tau=0.70$), melt energy ($r=0.90$, $\tau=0.67$), and
208 proglacial discharge ($r=0.88$, $\tau=0.71$) (Figure 4, Table S4). We find moderately strong
209 correlations with ice surface ablation ($r=0.74$, $\tau=0.59$) and air temperature ($r=0.70$, $\tau=0.54$),
210 drivers of melt energy and runoff, respectively. Lowest correlation is found for detrended ice
211 surface elevation (i.e. uplift, $r=0.36$, $\tau=0.24$, Table S4; Figure 4e). All correlations are

212 statistically significant ($p < 0.01$). Unlike melt energy (which turns negative, implying nocturnal
 213 refreezing), moulin input persists throughout the night. Because i) moulin input closely tracks
 214 (and derives from) melt energy; ii) virtually all surface runoff generated within Rio Behar
 215 catchment flows to its terminal moulin; and iii) an observed 6h time lag between peak melt
 216 energy and peak supraglacial discharge (**Table S3**) is similar to a previously calculated
 217 catchment routing delay for Rio Behar (i.e. estimated time-to-peak $t_p = 5.5$ h, *Smith et al., 2017*)
 218 we infer that supraglacial river discharge, a product of catchment-integrated melt energy, is the
 219 dominant supraglacial forcing variable driving our locally recorded ice speed variations.



220
 221 **Figure 4. Correlations between ice speed and other variables, after correcting for their mean differences (values**
 222 **in parentheses) in daily peak timing: (a) melt energy (-7h); (b) air temperature (-8h); (c) ablation (-4h); (d) moulin**
 223 **input (-2h); (e) ice surface elevation (+6h); (f) proglacial discharge (-2h at terminus). Statistical correlations**
 224 **presented in Table S4. Moulin input displays strongest correlation with ice speed ($r=0.90$, $\tau=0.70$, $p<0.01$).**

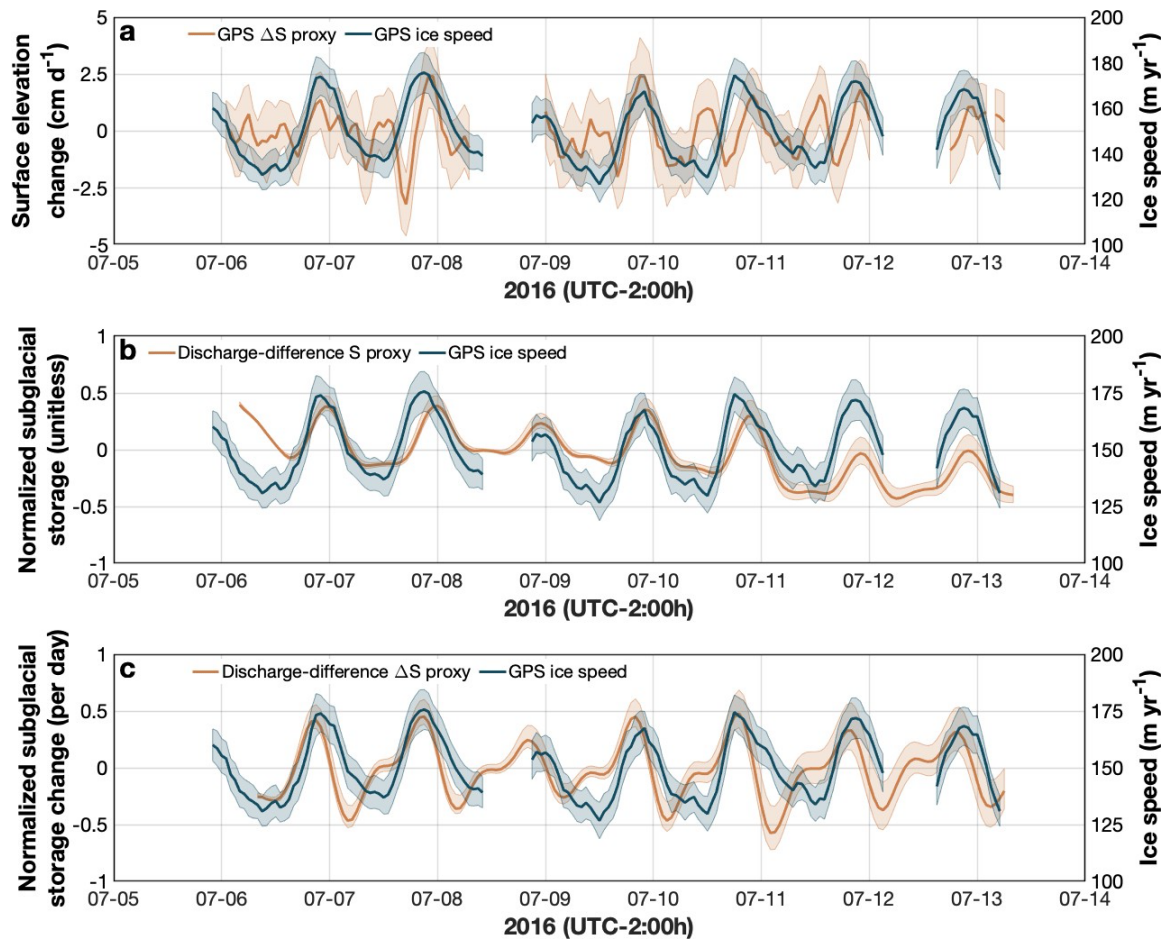
225

226 3.2 Comparison of short-term ice accelerations with S and ΔS

227 To further investigate drivers of short-term ice speed variations, we test proxies of
 228 subglacial water storage S and rate-of-change L/S calculated from GPS-derived ice surface
 229 observations (following *Anderson et al., 2004; Harper et al., 2007; Howat et al., 2008; Hoffman*
 230 *et al., 2011; Cowton et al., 2016; Andrews et al., 2018*) and by differencing normalized
 231 hydrographs of supraglacial and proglacial river discharge (**Text S7-S9**). Implicit in the latter
 232 "discharge-difference" calculations are assumptions that englacial storage is negligible; that
 233 en/subglacial melting is negligible; that subglacial routing delays are irrelevant to instantaneous
 234 net storage; and that proglacial discharge reflects overall regional basal water pressure, allowing

235 Rio Behar moulin input to be compared with regional proglacial discharge despite its smaller
 236 spatial domain (60 km² vs. ~2800 km² to 1750 m a.s.l.) and absolute discharge magnitude (~6-38
 237 m³ s⁻¹ vs. ~800-1300 m³ s⁻¹).

238 Comparison of our observed horizontal ice speeds with both proxies for *S* and *L'S*
 239 suggests that *L'S* drives short-term accelerations in ice speed (**Figures 5, S11, S13, S14; Table**
 240 **S5**). This conclusion is clearest from the discharge-difference proxies, with *L'S* tracking ice as
 241 well or better than *S* (see **Figure 5c vs. 5b; S13c vs. S13b; S11, S14**). This same conclusion
 242 may be drawn, albeit less compellingly, from conventional GPS-derived *S* and *L'S* proxies
 243 (**Figure 5a vs. Figure 2c; S11d and S14d vs. b**). For both methods, *L'S* generally correlates
 244 with ice accelerations better than *S* (**Table S5**) suggesting that changes in subglacial water
 245 storage force short-term ice speed accelerations at our field site.



246
 247 **Figure 5. Comparison of horizontal ice speed (blue) with proxies for subglacial water storage (*S*) and storage rate-**
 248 **of-change (ΔS): (a) ΔS estimated from GPS-derived ice surface elevation; (b) *S* estimated from normalized**
 249 **discharge-difference; (c) ΔS estimated from normalized discharge-difference. See Figure 2(c) for *S* estimated**
 250 **from GPS. Brief accelerations in ice speed track ΔS better than *S*. Discharge-difference (c) tracks ice speed better**
 251 **than GPS (a). Figure S13 presents another version of this figure using AK4 proglacial discharges.**

252 4. Discussion and conclusion

253 We find that diurnal cycles in moulin input (following the integrative and delaying
254 effects of surface routing through the upstream catchment) are the primary driver of short-term
255 accelerations in ice sliding velocity at our field site (**Figure 4**). This finding supports previous
256 work (*Andrews et al., 2014*) and the conclusion that over diurnal scales, variability in
257 supraglacial river input imposes a first-order control on subglacial water pressure fluctuations.
258 Furthermore, while short-term accelerations in ice speed closely follow moulin input, they also
259 tend to track proxies of subglacial water storage change (L'S) better than proxies of absolute
260 storage (S) (**Figures 5, S11, S13, S14**), suggesting that nightly peaks in subglacial water storage
261 drive subglacial basal pressure and short-term ice motion.

262 This conclusion is more evident in discharge-difference proxies than conventional GPS-
263 derived proxies (e.g. **Figures 5c vs. 5a; S13c vs. S13a; S11, S14**). This is likely due to our
264 inability to assess the impact of changes in the ice column due to variations in vertical strain,
265 making our GPS-derived proxies susceptible to local and non-local forcings (e.g., *Price et al.,*
266 *2008; Ryser et al., 2014*; see **Text S7**). Differencing supra- and proglacial hydrographs,
267 therefore, may characterize subglacial water storage conditions more sensitively than small
268 vertical ice surface elevation changes, which are inherently difficult to detect and have multiple
269 sources of uncertainty (*Anderson et al., 2004; Andrews et al., 2018*). A discharge input-output
270 approach (e.g. *Bartholomew et al., 2008; 2011; McGrath et al., 2011; Armstrong and Anderson,*
271 *2020*), comparing moulin inputs with proglacial outputs, offers an alternate strategy for
272 characterizing subglacial water storage and its link to basal sliding laws. Future studies, for
273 example, could develop discharge-difference proxies over longer time scales and larger study
274 areas by pairing surface-routed climate model output (e.g. *Smith et al., 2017; Yang et al., 2019*)
275 with proglacial discharge records (*Rennermalm et al. 2017; van As et al., 2019*), to relate net
276 increases/decreases in L'S to regional ice speed variations.

277 It is well-known that evolution of the subglacial system from inefficient to efficient states
278 acts to modulate the ice dynamical response to supraglacial water inputs (e.g. *Bartholomew et*
279 *al., 2010; 2011; Hoffman et al., 2011*). We find that peak or ascendant L'S is associated with
280 localized GrIS velocity accelerations (**Figure 5c; Figure 13c**). This suggests that highest
281 subglacial water pressure (and ice sliding speed) occurs when subglacial cavities are growing the
282 fastest, not when their volume is largest (e.g. *Iken et al., 1983; Cowton et al., 2016*). As such,
283 steady-state theoretical basal sliding laws – which assume a relationship between cavity size and
284 subglacial pressure – do not accurately represent transient behavior of the subglacial system.

285 It is important to note that the strong correlation between moulin input and ice velocity
286 reported here (**Figure 4d**) is unlikely to hold over an entire melt season. Previous work has
287 clearly established that Greenland ice sliding velocities are strongly influenced by long-term
288 seasonal evolution of the subglacial hydrological system (e.g. *Bartholomew et al., 2010;*
289 *Hoffman et al., 2011; Nienow et al., 2017; Andrews et al., 2018*). Our short 7-day record
290 captures neither the early nor late melt season, when subglacial efficiency (and associated ice
291 speeds) undergo extensive changes. Subglacial evolution makes melt-driven proxies
292 inappropriate for estimating ice motion over the entire melt season (*Bartholomew et al., 2010;*
293 *Andrews et al., 2014*) or multiple years (*Tedstone et al., 2015; Davison et al., 2019*). Over short
294 time scales, however, we find that diurnal cycles in moulin input are the primary driver of

295 fluctuating subglacial water pressures and associated ice accelerations – even in relatively thick
296 ice (~1 km) more than 40 km inland from the ice edge. Some slight differences in peak timings
297 between L'S and ice motion, as well as some non-linear behavior on descending limbs (**Figure**
298 **5c**, **Figure 13c**) are discussed further in **Text S9**.

299 This study adds to a small but growing collection of GrIS supraglacial streamflow
300 measurements (*Holmes 1955; Echelmeyer and Harrison 1990; Carver et al. 1994; McGrath et*
301 *al. 2011; Chandler et al., 2013; Gleason et al. 2016; Smith et al., 2015; 2017*). With peak daily
302 discharges of 26.59 – 37.61 m³/s (**Table S2**), the discharges reported here are far larger than
303 those collected in most supraglacial streams, but are typical for trunk supraglacial rivers in
304 southwest Greenland (*Smith et al., 2015; 2017*). Nearly all of them terminate in moulins (*Smith*
305 *et al., 2015; Yang and Smith, 2016*), and the high diurnal variability we observe (19.05 – 30.50
306 m³/s, **Table S2**) signifies that their subglacial channels are likely out of equilibrium with
307 supraglacial inputs for large portions of the day, such that associated accelerations in ice speed
308 are driven by addition or removal of water outside of the channelized system.

309 Based on satellite mapping (e.g. *Yang and Smith, 2013; 2016; Lampkin and VanderBerg,*
310 *2014; Smith et al., 2015; Yang et al., 2015; 2016*) and topographic modeling (e.g. *Banwell et al.*
311 *2012; 2016; Karlstrom and Yang, 2016; King et al., 2016; Crozier et al., 2018*), we maintain that
312 supraglacial rivers likely drive ice accelerations near hundreds of other terminal moulins as well.
313 Process-level understanding and modeling of subglacial hydrology and associated ice dynamics
314 should presume large, strongly diurnal inputs of meltwater entering hundreds of supraglacial
315 river moulins distributed throughout Greenland's ablation zone. These inputs, countered by
316 water output discharged beneath outlet glaciers, trigger short-term fluctuations in subglacial
317 water storage that drive short-term accelerations in ice sheet motion.

318

319 **5. Data Availability**

320 Discharge data, surface mass balance data, ADCP and GPS data summaries, S and ΔS
321 proxies, and a time-lapse camera video are available as tables (**Tables S1-S2**) and/or Additional
322 Supporting Information (**Datasets S1-S7**). Original, full-resolution ADCP and GPS data will be
323 archived at the Arctic Data Center (<https://doi.org/10.18739/A2PN8XG5T>). PROMICE
324 KAN_M automated weather station data (*Fausto and van As, 2019*) are available from
325 <https://www.promice.org/PromiceDataPortal/>. Proglacial river discharges for Qinguata
326 Kuussua/Watson River (*van As et al., 2019*), Akuliarusiarsuup Kuua (*Rennermalm et al., 2013b;*
327 *2017*), and Leverett Glacier (*Tedstone et al., 2017*) are available from
328 https://doi.org/10.22008/promice/data/watson_river_discharge ,
329 <https://doi.org/10.1594/PANGAEA.876357>, and [https://doi.org/10.5285/17c400f1-ed6d-4d5a-](https://doi.org/10.5285/17c400f1-ed6d-4d5a-a51f-aad9ee61ce3d)
330 [a51f-aad9ee61ce3d](https://doi.org/10.5285/17c400f1-ed6d-4d5a-a51f-aad9ee61ce3d).

331

332 **6. Acknowledgements**

333 This research was funded by the NASA Cryospheric Science Program (grants
334 80NSSC19K0942 and NNX14AH93G) managed by Dr. Thorsten Markus. Polar Field Services,

335 Inc. and Kangerlussuaq International Science Support (KISS) provided logistical field support.
336 GPS equipment was loaned by UNAVCO, Inc. with support from NASA and NSF. A. Zaino and
337 J. Pettit of UNAVCO advised on GPS receiver hardware, programming, and installation.
338 Proglacial discharge data from Qinguata Kuussua/Watson River were gathered by the
339 University of Copenhagen and the Geological Survey of Denmark and Greenland. The KAN_M
340 weather station is part of the Programme for Monitoring of the Greenland Ice Sheet
341 (www.PROMICE.dk). The authors declare there are no real or perceived financial conflicts of
342 interest, or other affiliations for any author that may be perceived as having a conflict of interest
343 with respect to the results of this research.

344

345 **Dedication**

346 We dedicate this paper to the memory of Dr. Konrad Steffen (1952-2020).

347

348 **References**

349

- 350 Andrews L.C., Catania G.A., Hoffman M.J., Gulley J.D., Lüthi M.P., et al. (2014), Direct
351 observations of evolving subglacial drainage beneath the Greenland Ice Sheet. *Nature*, 514,
352 80–83, <https://doi.org/10.1038/nature13796>
- 353 Andrews, L.C., Hoffman, M.J., Neumann, T.A., Catania, G.A., Lüthi, M.P., Hawley, R.L., et al.
354 (2018), Seasonal evolution of the subglacial hydrologic system modified by supraglacial
355 lake drainage in western Greenland. *Journal of Geophysical Research-Earth Surface*, 123,
356 1479–1496. <https://doi.org/10.1029/>
- 357 Anderson, R.S., Anderson, S.P., MacGregor, K.R., Waddington, E.D., O'Neel, S., Riihimaki,
358 C.A., Loso, M.G. (2004), Strong feedbacks between hydrology and sliding of a small
359 alpine glacier. *Journal of Geophysical Research—Earth Surface*, 109(F3), F03005.
360 <https://doi.org/10.1029/2004JF000120>
- 361 Armstrong, W.H., Anderson, R.S. (2020), Ice-marginal lake hydrology and the seasonal
362 dynamical evolution of Kennicott Glacier, Alaska. *Journal of Glaciology*, 66(259), 699-
363 713. <https://doi.org/10.1017/jog.2020.41>
- 364 Banwell, A.F., Arnold, N.S., Willis, I.C., Tedesco, M., Ahlstrom, A.P. (2012), Modelling
365 supraglacial water routing and lake filling on the Greenland ice sheet. *J. Geophys. Res.*,
366 117, F04012, doi:10.1029/2012JF002393.
- 367 Banwell, A., Hewitt, I., Willis, I., Arnold, N. (2016), Moulin density controls drainage
368 development beneath the Greenland ice sheet. *J. Geophys. Res. Earth Surf.*, 121, 2248–
369 2269, doi:10.1002/2015JF003801.
- 370 Bartholomaeus, T.C, Anderson, R.S., Anderson, S.P. (2008), Response of glacier basal motion to
371 transient water storage. *Nature Geoscience*, 1, 33–37. <https://doi.org/10.1038/ngeo.2007.52>

- 372 Bartholomew, T.C., Anderson, R.S., Anderson, S.P. (2011), Growth and collapse of the
373 distributed subglacial hydrologic system of Kennicott Glacier, Alaska, USA, and its effects
374 on basal motion. *Journal of Glaciology*, 57(206), 985-1002, DOI:
375 <https://doi.org/10.3189/002214311798843269>
- 376 Bartholomew, I., Nienow, P., Mair, D. et al. (2010), Seasonal evolution of subglacial drainage
377 and acceleration in a Greenland outlet glacier. *Nature Geosci.*, 3, 408–411,
378 <https://doi.org/10.1038/ngeo863>
- 379 Bartholomew, I., Nienow, P., Sole, A., Mair, D., Cowton, T., Palmer, S., Wadham, J. (2011),
380 Supraglacial forcing of subglacial drainage in the ablation zone of the Greenland ice sheet.
381 *Geophys. Res. Lett.*, 38, L08502, doi:10.1029/2011GL047063.
- 382 Bartholomew, I. D., Nienow, P., Sole, A., Mair, D., Cowton, T., King, M. A. (2012), Short-term
383 variability in Greenland Ice Sheet motion forced by time-varying meltwater drainage:
384 Implications for the relationship between subglacial drainage system behavior and ice
385 velocity. *Journal of Geophysical Research: Earth Surface*, 117(F3), F03002.
386 <https://doi.org/10.1029/2011JF002220>
- 387 Bell, R. (2008) The role of subglacial water in ice-sheet mass balance. *Nature Geosci*, 1, 297–
388 304, <https://doi.org/10.1038/ngeo186>
- 389 Bindschadler, R. (1983), The importance of pressurized subglacial water in separation and
390 sliding at the glacier bed. *Journal of Glaciology*, 29(101), 3–19.
391 <https://doi.org/10.3189/S0022143000005104>
- 392 Burkey, J. (2021). Mann-Kendall Tau-b with Sen's Method (enhanced). *MATLAB Central File*
393 *Exchange*, [https://www.mathworks.com/matlabcentral/fileexchange/11190-mann-kendall-](https://www.mathworks.com/matlabcentral/fileexchange/11190-mann-kendall-tau-b-with-sen-s-method-enhanced)
394 [tau-b-with-sen-s-method-enhanced](https://www.mathworks.com/matlabcentral/fileexchange/11190-mann-kendall-tau-b-with-sen-s-method-enhanced), retrieved 10 January 2021
- 395 Carver S., Sear D., Valentine E. (1994) An observation offroll waves in a supraglacial meltwater
396 channel, Harlech Gletscher, East Greenland. *J. Glaciology* 40(134):75–78
- 397 Catania G.A., Neumann T.A. (2010), Persistent englacial drainage features in the Greenland Ice
398 Sheet. *Geophys. Res. Lett.*, 37:1–5, <https://doi.org/10.1029/2009GL041108>
- 399 Chandler, D. M., Wadham, J. L., Lis, G. P., Cowton, T., Sole, A., Bartholomew, I., ... Hubbard,
400 A. (2013), Evolution of the subglacial drainage system beneath the Greenland Ice Sheet
401 revealed by tracers. *Nature Geoscience*, 6(3), 195–198. <https://doi.org/10.1038/ngeo1737>
402
- 403 Chen, G. (1998). GPS kinematic positioning for airborne laser altimetry at Long Valley,
404 California. Massachusetts Institute of Technology, Cambridge, MA. Retrieved from
405 <http://dspace.mit.edu/handle/1721.1/9680>
- 406 Christoffersen, P., Bougamont, M., Hubbard, A., Doyle, S.H., Grigsby, S., Pettersson, R. (2018),
407 Cascading lake drainage on the Greenland Ice Sheet triggered by tensile shock and fracture.
408 *Nature Communications* 9, 1064 (2018). <https://doi.org/10.1038/s41467-018-03420-8>
- 409 Chu, V. W. (2014), Greenland ice sheet hydrology: a review, *Prog. Phys. Geogr.*, 38(1), 19-54.
- 410 Chu W., Schroeder D.M., Seroussi H., Creyts T.T., Palmer S.J., Bell R.E. (2016), Extensive
411 winter subglacial water storage beneath the Greenland Ice Sheet. *Geophys. Res. Lett.*
412 43(24):12,484-12,492

- 413 Clason C.C., Mair D.W.F., Nienow P.W., Bartholomew I.D., Sole A., et al. (2015), Modelling
414 the transfer of supraglacial meltwater to the bed of Leverett Glacier, Southwest Greenland.
415 *The Cryosphere*, 9(1), 123–38. [www.the-cryosphere.net/9/123/2015/doi:10.5194/tc-9-123-](http://www.the-cryosphere.net/9/123/2015/doi:10.5194/tc-9-123-2015)
416 2015
- 417 Cooper M.G., Smith L.C., Rennermalm A.K., Miège C., Pitcher L.H., et al. (2018), Meltwater
418 storage in low-density near-surface bare ice in the Greenland ice sheet ablation zone. *The*
419 *Cryosphere* 12(3):955–70
- 420 Cooper, M.G., Smith, L.C. (2019) Satellite Remote Sensing of the Greenland Ice Sheet Ablation
421 Zone: A Review. *Remote Sensing*, 11, 2405. DOI: 10.3390/rs11202405
- 422 Cowton T., Nienow P., Sole A., Wadham J., Lis G., et al. (2013), Evolution of drainage system
423 morphology at a land-terminating Greenlandic outlet glacier. *J. Geophys. Res. Earth Surf.*
424 118(1):29–41
- 425 Cowton, T., Nienow, P., Sole, A., Bartholomew, I., Mair, D. (2016), Variability in ice motion at
426 a land-terminating Greenlandic outlet glacier: the role of channelized and distributed
427 drainage systems. *Journal of Glaciology*, doi:10.1017/jog.2016.36
- 428 Crozier, J., Karlstrom, L., and Yang, K. (2018), Basal control of supraglacial meltwater
429 catchments on the Greenland Ice Sheet, *The Cryosphere*, 12, 3383–3407,
430 <https://doi.org/10.5194/tc-12-3383-2018>
- 431 Davison, B.J., Sole, A.J., Livingstone, S.J., Cowton, T.R., Nienow, P.W. (2019) The influence of
432 hydrology on the dynamics of land-terminating sectors of the Greenland ice sheet.
433 *Frontiers in Earth Science*, 7(10), ISSN 2296-6463
434 <https://doi.org/10.3389/feart.2019.00010>
- 435 Echelmeyer K., Harrison W.D. (1990) Jakobshavns Isbræ, West Greenland: seasonal variations
436 in velocity—or lack thereof. *J. Glaciology*, 36(122):82–88.
- 437
- 438 Estey, L.H., and Meertens, C.M. (1999) TEQC: The Multi-Purpose Toolkit for GPS/GLONASS
439 Data. *GPS Solutions* (pub. by John Wiley & Sons), Vol. 3(1), 42-49,
440 <https://doi.org/10.1007/PL00012778>
- 441 Fausto, R.S. and van As, D., (2019). Programme for monitoring of the Greenland ice sheet
442 (PROMICE): Automatic weather station data. Version: v03, Dataset published via
443 Geological Survey of Denmark and Greenland. DOI:
444 <https://doi.org/10.22008/promice/data/aws>
- 445 Flowers, G., Jarosch, A., Belliveau, P., Fuhrman, L. (2016), Short-term velocity variations and
446 sliding sensitivity of a slowly surging glacier. *Annals of Glaciology*, 57(72), 71-83.
447 doi:10.1017/aog.2016.7
- 448 Flowers, G.E. (2018), Hydrology and the future of the Greenland Ice Sheet. *Nature*
449 *Communications*, 9(2729). DOI: 10.1038/s41467-018-05002-0
- 450 Gagliardini, O., Cohen, D., Raback, P. Zwinger, T. (2007) Finite-element modeling of subglacial
451 cavities and related friction law. *J. Geophys. Res.* 112, F02027.

- 452 Gleason, C.J., Smith, L.C., Chu, V.W., Legleiter, C.J., Pitcher, L.H., Overstreet, B.T.,
453 Rennermalm, A.K., Forster, R.R., and Yang, K. (2016), Characterizing supraglacial
454 meltwater channel hydraulics on the Greenland Ice Sheet from in situ observations. *Earth*
455 *Surf. Process. Landforms*, 41: 2111– 2122. doi: 10.1002/esp.3977.
- 456 Harper, J. T., Humphrey, N. F., Pfeffer, W. T., Lazar, B. (2007), Two modes of accelerated
457 glacier sliding related to water. *Geophysical Research Letters*, 34(12), L12503.
458 <https://doi.org/10.1029/2007GL030233>
- 459 Hoffman M.J., Catania G.A., Neumann T.A., Andrews L.C., Rumrill J.A. (2011), Links between
460 acceleration, melting, and supraglacial lake drainage of the western Greenland Ice Sheet. *J.*
461 *Geophys. Res.*, 116, F04035
- 462 Hoffman, M., Andrews, L., Price, S. et al. (2016), Greenland subglacial drainage evolution
463 regulated by weakly connected regions of the bed. *Nature Communications*, 7, 13903.
464 <https://doi.org/10.1038/ncomms13903>
- 465 Holmes G. 1955. Morphology and hydrology of the Mint Julep area, southwest Greenland. In
466 Project Mint Julep: Investigation of Smooth Ice Areas of the Greenland Ice Cap, 1953; Part
467 II: Special Scientific Reports. Maxwell Air Force Base, AL: Arct. Desert Tropic Inf. Cent.,
468 Res. Stud. Inst., Air Univ.
- 469 Howat, I.M., Tulaczyk, S., Waddington, E., Björnsson, H. (2008), Dynamic controls on glacier
470 basal motion inferred from surface ice motion. *Journal of Geophysical Research: Earth*
471 *Surface*, 113(F3), F03015. <https://doi.org/10.1029/2007JF000925>
- 472 Iken, A. Röthlisberger, H., Flotron, A., W. Haeberli, W. (1983) The uplift of Unteraargletscher at
473 the beginning of the melt season - a consequence of water storage at the bed? *J. Glaciol.*,
474 29(101), 28–47
- 475 Irvine-Fynn, T.D.L., A.J. Hodson, B.J. Moorman, G. Vatne, A.L. Hubbard (2011), Polythermal
476 glacier hydrology: a review, *Rev. Geophys.*, 49(4), RG4002.
- 477 Jansson, P. (1996), Dynamics and hydrology of a small polythermal valley glacier. *Geografiska*
478 *Annaler: Series A, Physical Geography*, 78, 171–180.
- 479 Kamb, B. (1970), Sliding motion of glaciers: Theory and observation. *Reviews of Geophysics*,
480 8(4), 673–728. <https://doi.org/10.1029/RG008i004p00673>
- 481 Karlstrom, L., Yang, K. (2016), Fluvial supraglacial landscape evolution on the Greenland Ice
482 Sheet, *Geophys. Res. Lett.*, 43, 2683– 2692, doi:10.1002/2016GL067697.
- 483 King L., Hassan M.A., Yang K., Flowers G. (2016), Flow Routing for Delineating Supraglacial
484 Meltwater Channel Networks. *Remote Sensing*, 8(12):988. doi:10.3390/rs8120988
- 485 Lampkin, D.J., VanderBerg, J. (2014), Supraglacial melt channel networks in the Jakobshavn
486 Isbræ region during the 2007 melt season, *Hydrol. Process.*, 28, 6038– 6053, doi:
487 10.1002/hyp.10085
- 488 Lindbäck, K., Pettersson, R., Hubbard, A.L., Doyle, S.H., van As, D., Mikkelsen, A.B.,
489 Fitzpatrick, A.A. (2015). Subglacial water drainage, storage, and piracy beneath the
490 Greenland Ice Sheet. *Geophysical Research Letters*, 42(18), 7606–7614.
491 <https://doi.org/10.1002/2015GL065393>

- 492 Mair, D., Sharp, M.J., Willis, I.C. (2002), Evidence for basal cavity opening from analysis of
 493 surface uplift during a high-velocity event: Haut Glacier d'Arolla, Switzerland. *Journal of*
 494 *Glaciology*, 48(161), 208–216. <https://doi.org/10.3189/172756502781831502>
- 495 McGrath D., Colgan W., Steffen K., Lauffenburger P., Balog J. (2011), Assessing the summer
 496 water budget of a moulin basin in the Sermeq Avannarleq ablation region, Greenland ice
 497 sheet. *J. Glaciol.* 57(205):954–64
- 498 Meierbachtol, T., J. Harper, N. Humphrey (2013), Basal Drainage System Response to
 499 Increasing Surface Melt on the Greenland Ice Sheet. *Science*, 341, 6147, 777-779. DOI:
 500 10.1126/science.1235905
- 501 Morlighem, M., Williams, C. N., Rignot, E., An, L., Arndt, J. E., Bamber, J. L., ... Zinglensen,
 502 K. B. (2017), BedMachine v3: Complete bed topography and ocean bathymetry mapping of
 503 Greenland from multibeam echo sounding combined with mass conservation, *Geophysical*
 504 *Research Letters*, 44, 11,051– 11,061. <https://doi.org/10.1002/2017GL074954> [Data
 505 accessed 7/20 at Morlighem, M. et al. 2017, updated 2018. IceBridge BedMachine
 506 Greenland, Version 3. Boulder, Colorado USA. NASA National Snow and Ice Data Center
 507 Distributed Active Archive Center. doi: <https://doi.org/10.5067/2CIX82HUV88Y>]
- 508 Nienow, P.W., Sole, A.J., Slater, D.A., Cowton, T.R. (2017), Recent Advances in Our
 509 Understanding of the Role of Meltwater in the Greenland Ice Sheet System. *Curr Clim*
 510 *Change Rep* (2017) 3:330–344, DOI 10.1007/s40641-017-0083-9
- 511 Palmer S., Shepherd A., Nienow P., Joughin I. (2011), Seasonal speedup of the Greenland ice
 512 sheet linked to routing of surface water. *Earth Planet. Sci. Lett.* 302(3–4):423–28
- 513 Pitcher, L.H., Smith, L.C. (2019), Supraglacial Streams and Rivers. *Annual Review of Earth and*
 514 *Planetary Sciences*, 47(1), 421-452, <https://doi.org/10.1146/annurev-earth-053018-060212>
- 515 Pitcher, L.H., Smith, L.C., Gleason, C.J., Miede, C., Ryan, J.C., Hagedorn, B., van As, D., Chu,
 516 W., Forster, R.R. (2020), Direct observation of wintertime meltwater drainage from the
 517 Greenland Ice Sheet. *Geophysical Research Letters*, e2019GL086521,
 518 <https://doi.org/10.1029/2019GL086521>
- 519 Poinar, K., Joughin, I., Das, S. B., Behn, M. D., Lenaerts, J. T. M., and van den Broeke, M. R.
 520 (2015), Limits to future expansion of surface-melt-enhanced ice flow into the interior of
 521 western Greenland. *Geophysical Research Letters* 42, 1800–1807,
 522 <https://doi.org/10.1002/2015GL063192>
- 523 Price, S. F., Payne, A. J., Catania, G. A., & Neumann, T. A. (2008). Seasonal acceleration of
 524 inland ice via longitudinal coupling to marginal ice. *Journal of Glaciology*, 54(185), 213–
 525 219. <https://doi.org/10.3189/002214308784886117>
- 526 Rennermalm, Å.K., Moustafa, S.E., Mioduszewski, J., Chu, V.W., Forster, R.R., Hagedorn, B.,
 527 Harper, J.T., Mote, T.L., Robinson, D.A., Shuman, C.A., et al. (2013a), Understanding
 528 Greenland ice sheet hydrology using an integrated multi-scale approach. *Environ. Res. Lett.*
 529 2013, 8, 015017.
- 530 Rennermalm, Å.K., Smith, L. C., Chu, V.W., Box, J.E., Forster, R.R., Van den Broeke, M. R.
 531 (2013b), Evidence of meltwater retention within the Greenland ice sheet. *The Cryosphere*,
 532 7, 1433–1445, 2013. <https://doi.org/10.5194/tc-7-1433-2013>

- 533 Rennermalm, A.K., Smith, L.C., Hammann, A.C., Leidman, S.Z., Cooper, M.G., Cooley, S.W.,
534 Pitcher, L. (2017), River discharge at station AK-004-001, 2008 - 2016, version 3.0. The
535 State University of New Jersey, *PANGAEA*, <https://doi.org/10.1594/PANGAEA.876357>
- 536 Ryan, J.C., Smith, L.C., van As, D., Cooley, S.W., Cooper, M.G., Pitcher, L.H, Hubbard, A.
537 (2019), Greenland Ice Sheet surface melt amplified by snowline migration and bare ice
538 exposure *Science Advances* 5(3), eaav3738, DOI: 10.1126/sciadv.aav3738
- 539 Ryser, C., Lüthi, M. P., Andrews, L. C., Catania, G. A., Funk, M., Hawley, R. L., et al. (2014).
540 Caterpillar-like ice motion in the ablation zone of the Greenland ice sheet. *Journal of*
541 *Geophysical Research: Earth Surface*, 119(10), 2258–2271.
542 <https://doi.org/10.1002/2013JF003067>
- 543 Schoof, C. (2010), Ice-sheet acceleration driven by melt supply variability. *Nature*.
544 468(7325):803
- 545 Schoof, C. (2005), The effect of cavitation on glacier sliding. *Proc. R. Soc. A*. 461609–627
546 <http://doi.org/10.1098/rspa.2004.1350>.
- 547 Schweizer, J., Iken, A. (1992), The role of bed separation and friction in sliding over an
548 undeformable bed. *Journal of Glaciology*, 38(128), 77–92.
549 <https://doi.org/10.3189/S0022143000009618>
- 550 Stevens, L., Behn, M., McGuire, J., Das, S.B., Joughin, I., Herring, T., Shean, D.E., King, M.A
551 (2015), Greenland supraglacial lake drainages triggered by hydrologically induced basal
552 slip. *Nature* 522, 73–76. <https://doi.org/10.1038/nature14480>
- 553 Sugiyama, S., Gudmundsson, H. (2004), Short-term variations in glacier flow controlled by
554 subglacial water pressure at Lauteraargletscher, Bernese Alps, Switzerland. *Journal of*
555 *Glaciology*, 50(170), 353–362. <https://doi.org/10.3189/172756504781829846>
- 556 Shepherd, A., Hubbard, A., Nienow, P., King, M., McMillan, M., Joughin, I. (2009), Greenland
557 ice sheet motion coupled with daily melting in late summer, *Geophys. Res. Lett.*, 36,
558 L01501, doi:10.1029/2008GL035758.
- 559 Smith, L.C., Chu, V.W., Yang, K., Gleason, C.J., Pitcher, L.H., Rennermalm, Å.K., et al. (2015),
560 Efficient meltwater drainage through supraglacial streams and rivers on the southwest
561 Greenland Ice Sheet. *Proceedings of the National Academy of Sciences*, 112 (4) 1001-1006.
562 <https://doi.org/10.1073/pnas.1413024112>
- 563 Smith, L.C., Yang, K., Pitcher, L.H., Overstreet, B.T., Chu, V.W., Rennermalm, Å.K., et al.
564 (2017), Direct measurements of meltwater runoff on the Greenland Ice Sheet surface.
565 *Proceedings of the National Academy of Sciences*, 114(50), E10622-E10631, DOI:
566 10.1073/pnas.1707743114
- 567 Tedesco, M., Fettweis, X., Mote, T., Wahr, J., Alexander, P., Box, J.E., and Wouters, B. (2013),
568 Evidence and analysis of 2012 Greenland records from spaceborne observations, a regional
569 climate model and reanalysis data, *The Cryosphere*, 7, 615–630, [https://doi.org/10.5194/tc-](https://doi.org/10.5194/tc-7-615-2013)
570 [7-615-2013](https://doi.org/10.5194/tc-7-615-2013)
- 571 Tedstone, A.J., Nienow, P.W., Sole, A.J., Mair, D.W.F., Cowton, T.R., Bartholomew, I.D., King,
572 M.A. (2013), Greenland ice sheet motion insensitive to exceptional meltwater forcing.

573 *Proceedings of the National Academy of Sciences*, 110 (49) 19719-19724; DOI:
574 10.1073/pnas.1315843110

575 Tedstone, A., Nienow, P., Gourmelen, N., Dehecq, A., Goldberg, D., Hanna, E. (2015), Decadal
576 slowdown of a land-terminating sector of the Greenland Ice Sheet despite warming.
577 *Nature*, 526, 692–695. <https://doi.org/10.1038/nature15722>

578 Tedstone, A.J. et al (2017), Proglacial discharge measurements, Leverett Glacier, south-west
579 Greenland (2009-2012), Polar Data Centre, Natural Environment Research Council, UK.
580 <https://doi.org/10.5285/17c400f1-ed6d-4d5a-a51f-aad9ee61ce3d>

581 van As, D., Bech Mikkelsen, A., Holtegaard Nielsen, M., Box, J. E., Claesson Liljedahl, L.,
582 Lindbäck, K., Pitcher, L., Hasholt, B. (2017), Hypsometric amplification and routing
583 moderation of Greenland ice sheet meltwater release. *The Cryosphere*, 11, 1371–1386,
584 <https://doi.org/10.5194/tc-11-1371-2017>

585 van As, D., Hasholt, B., Ahlstrøm, A.P., Box, J.E., Cappelen, J., Colgan, W., Fausto, R.S.,
586 Mernild, S.H., Mikkelsen, A.B., Noël, B.P.Y., Petersen, D., van den Broeke, M.R. (2018),
587 Reconstructing Greenland Ice Sheet meltwater discharge through the Watson River (1949–
588 2017), *Arctic, Antarctic, and Alpine Research*, 50:1, DOI:
589 10.1080/15230430.2018.1433799

590 van As, D., Hasholt, B., Ahlstrøm, A. P., Box, J. E., Cappelen, J., Colgan, W., Fausto, R.S.,
591 Mernild, S.H., Mikkelsen, A.P., Noël, B.P.Y., Petersen, D., van den Broeke, M. R. (2019).
592 Programme for monitoring of the Greenland ice sheet (PROMICE): Watson river
593 discharge. Version: v01, Dataset published via Geological Survey of Denmark and
594 Greenland. https://doi.org/10.22008/promice/data/watson_river_discharge

595 van de Wal, R. S. W., W. Boot, M. R. Van den Broeke, C. J. P. P. Smeets, C. H. Reijmer, J. J. A.
596 Donker, J. Oerlemans (2008), Large and rapid melt-induced velocity changes in the
597 ablation zone of the Greenland ice sheet, *Science*, 321(5885), 111-113.

598 van de Wal, R.S.W., Smeets, C.J.P.P., Boot, W., Stoffelen, M., van Kampen, R., Doyle, S.H.,
599 Wilhelms, F., van den Broeke, M.R., Reijmer, C.H., Oerlemans, J., Hubbard, A. (2015),
600 Self-regulation of ice flow varies across the ablation area in south-west Greenland, *The*
601 *Cryosphere*, 9, 603–611, <https://doi.org/10.5194/tc-9-603-2015>

602 Williams, J.J., Gourmelen, N., Nienow, P. (2020), Dynamic response of the Greenland ice sheet
603 to recent cooling. *Sci Rep*, 10, 1647. <https://doi.org/10.1038/s41598-020-58355-2>

604 Yang, K., Smith, L.C., Supraglacial Streams on the Greenland Ice Sheet Delineated From
605 Combined Spectral-Shape Information in High-Resolution Satellite Imagery. *IEEE*
606 *Geoscience and Remote Sensing Letters*, 10(4), 801–805,
607 doi:10.1109/LGRS.2012.2224316, 2013

608 K. Yang, Smith, L.C., Chu, V.W., Gleason, C.J., Li, M. (2015), A Caution on the Use of Surface
609 Digital Elevation Models to Simulate Supraglacial Hydrology of the Greenland Ice Sheet.
610 *IEEE Journal of Selected Topics in Applied Earth Observations and Remote Sensing*,
611 8(11), 5212-5224, doi: 10.1109/JSTARS.2015.2483483.

612 Yang K., Smith L.C. (2016), Internally drained catchments dominate supraglacial hydrology of
613 the southwest Greenland Ice Sheet. *J. Geophys. Res. Earth Surf.*, 1891–1910.
614 doi:10.1002/2016JF003927

- 615 Yang, K., Smith, L.C., Karlstrom, L., Cooper, M.G., Tedesco, M., van As, D., Cheng, X., Chen,
616 Z., Li, M.(2018), A new surface meltwater routing model for use on the Greenland Ice
617 Sheet surface, *The Cryosphere*, 12, 3791–3811, <https://doi.org/10.5194/tc-12-3791-2018>
- 618 Yang, K., Smith, L.C., Fettweis, X., Gleason, C.J., Lu, Y., Li, M. (2019) Surface meltwater
619 runoff on the Greenland ice sheet estimated from remotely sensed supraglacial lake
620 infilling rate (2019). *Remote Sensing of Environment*, 234, 111459,
621 <https://doi.org/10.1016/j.rse.2019.111459>
- 622 Yang, K., Sommers, A., Andrews, L.C., Smith, L. C., Lu, X., Fettweis, X., Li, M. (2020) Inter-
623 comparison of surface meltwater routing models for the Greenland Ice Sheet and influence
624 on subglacial effective pressures, *The Cryosphere Discuss.*, [https://doi.org/10.5194/tc-](https://doi.org/10.5194/tc-2019-255)
625 [2019-255](https://doi.org/10.5194/tc-2019-255).
- 626 Zwally, H.J., Abdalati, W., Herring, T., Larson, K., Saba, J., Steffen, K. (2002), Surface melt
627 induced acceleration of Greenland ice-sheet flow, *Science*, 297(5579), 218-222. DOI:
628 [10.1126/science.1072708](https://doi.org/10.1126/science.1072708)
- 629
- 630